




Article

# Performance Evaluation of MQL Parameters Using $\text{Al}_2\text{O}_3$ and $\text{MoS}_2$ Nanofluids in Hard Turning 90CrSi Steel

Tran Minh Duc <sup>1</sup>, Tran The Long <sup>1,\*</sup>  and Tran Quyet Chien <sup>2</sup>

<sup>1</sup> Department of Manufacturing Engineering, Faculty of Mechanical Engineering, Thai Nguyen University of Technology, Thai Nguyen 250000, Vietnam; minhduc@tnut.edu.vn

<sup>2</sup> Mechanical workshop, Thai Nguyen University of Technology, Thai Nguyen 250000, Vietnam; tranchien@tnut.edu.vn

\* Correspondence: tranthelong90@gmail.com or tranthelong@tnut.edu.vn; Tel.: +84-985-288-777

Received: 9 April 2019; Accepted: 1 May 2019; Published: 8 May 2019



**Abstract:** Hard machining has gained much attention to be an alternative solution for many traditional finish grinding operations due to high productivity, ease to adapt to complex part contours, the elimination of cutting fluids, good surface quality, and the reduction of machine tool investment. However, the enormous amount of heat generated from the cutting zone always requires the high-grade inserts and limits the cutting conditions. The MQL technique with nanofluids assisted for hard machining helps to improve the cutting performance while ensuring environmentally friendly characteristics. This paper focuses on the development of MQL technique by adding  $\text{Al}_2\text{O}_3$  and  $\text{MoS}_2$  nanoparticles to the base fluids (soybean oil and water-based emulsion) for the hard turning of 90CrSi steel (60÷62 HRC). The analysis of variance (ANOVA) is used to evaluate the performance of MQL parameters in terms of cutting forces and surface roughness. The study reveals that a better performance of coated carbide inserts is observed by using MQL with  $\text{Al}_2\text{O}_3$  and  $\text{MoS}_2$  nanofluids. In addition, the fluid type, nanoparticles and nanoparticle concentration have a strong effect on cutting performance. The interaction influence among the investigated variables is also studied in order to provide the technical guides for further studies using  $\text{Al}_2\text{O}_3$  and  $\text{MoS}_2$  nanofluids.

**Keywords:** hard turning; MQL; soybean oil; emulsion;  $\text{Al}_2\text{O}_3$  and  $\text{MoS}_2$  nanoparticles; nanofluid

## 1. Introduction

Metal cutting processes are industrial processes in which the metal parts are shaped by the removal of unwanted material. They are required for almost all products, so the conventional machining operations, such as turning, boring, drilling, and milling, are the most crucial part of the production. For the conventional approach, the solution to finishing hardened steel parts has been grinding, but this process still has some main drawbacks like low material removal rate, heat deterioration, and the negative effects of coolant usage for the environment. Recently, hard machining has been considered an alternative solution for many traditional finish grinding operations. It has gained much attention and can be defined as the machining operation of a workpiece with the hardness value typically in the 45–70 HRC range by directly using the tools with geometrically defined cutting edges [1]. A number of clear benefits have been observed for machining of hard parts with a cutting tool such as high productivity, ease to adapt to complex part contours, the elimination of cutting fluids, good surface quality, and the reduction of machine tool investment. However, the selection of the cutting-tool inserts that can ensure the proper tool life and high precision of the machining components always faces the challenge. In addition, the biggest question is whether the cooling and lubricating fluids are used or not because the thermal shock must be taken into account to avoid the breakage of the inserts. In the

earliest type of hard machining, the cutting processes without coolant gave out obvious cost benefits, but the high hardness materials and the enormous amount of generated heat demand the high-grade inserts such as coated carbide, ceramics, (P)CBN, PCD tools.

The WC/Co cemented carbide tools were developed for dry turning by coating with a thin wear resistant Ti55Al45N coating deposited by physical vapor deposition (PVD) method reported by K. Zhang et al. [2]. The obtained results showed that the cutting performance of nano-scale textured tools was improved when compared to that of un-textured tools. The reduction of contact length at tool–chip interface at rake face contributes to the decrease of friction coefficient, cutting forces, cutting temperature, and tool wear. Moreover, Liu, Y. et al. [3] investigated the femtosecond laser on the WC/Co carbide tools' flank face in dry cutting of green Al<sub>2</sub>O<sub>3</sub> ceramics, the difficult-to-cut material. The better wear resistance of the tools and an improvement of surface quality were achieved. C.S. Kumar and his co-authors investigated the dry cutting of hardened AISI 52100 steel (62 HRC) using Al<sub>2</sub>O<sub>3</sub>/TiCN composite ceramic inserts which were fabricated on the rake surface with microscale textures by WEDM process [4]. The reduced chip-tool contact length was also observed, and it contributed to superior anti-adhesion behavior when compared to the conventional cutting tool. In addition, the cutting temperatures during hard turning process are very high, ranging from 720 to 1050 °C with cutting speed 100–180 m/min when using different ceramic tools [5]. Su, Y. et al. [6] used the micro-textured polycrystalline diamond tool in dry turning of Ti6Al4V titanium alloy. The tribological properties of the tool–chip interface were better than that of the untextured PCD tools. The reduction of cutting force and tool-chip contact length were obtained by using micro-grooved PCD tools. Bouacha, K. et al. [7] studied surface roughness and cutting forces in hard turning of AISI 52100 bearing steel with CBN tool. The experiment results had shown that the thrust force has the highest value, and the surface roughness is highly affected by feed rate. The cutting forces increase along with the rise of feed rate, depth of cut and hardness, which also contribute to the higher wear rate of CBN tool. During dry cutting processes of hardened steels, the large amount of heat is generated, which would lead to thermal failure of cutting tools and the reduction of tool life. The cutting speed is limited due to the rise of cutting temperature. The part-thermal distortion, handling, and in-process gauging caused by high heat are necessarily considered. Thus, it is necessary to find the solution for decreasing the temperature in the cutting zone while ensuring the environmentally friendly characteristics of hard cutting processes.

Minimum quantity lubrication (MQL) has been developing to be an attractive alternative solution for flood and dry machining. The use of a small amount of cutting fluid in the form of an oil mist directly sprayed to the contact zone helps to reduce the friction coefficient significantly [1]. It contributes to the decrease of cutting forces, cutting temperature and tool wear as well as the improvement of surface quality and tool life [8–13]. However, the low cooling effect is the main drawback of MQL technology, so it does not work so well when applied to difficult-to-cut materials, especially for high hardness steels. The cutting tools usually suffer rapid wear rate caused by the enormous generated heat from cutting zone. To improve MQL technique assisted for hard machining, many studies have been made by following two approaches: (1) MQCL and (2) MQL using nanofluids. Among these, the nanofluids used in MQL have been a new research trend and gained much attention of the researchers around the world in recent years. The use of different types of nanoparticles, such as Al<sub>2</sub>O<sub>3</sub>, MoS<sub>2</sub>, SiO<sub>2</sub>, ZrO<sub>2</sub>, CNTs and diamond, reinforced in MQL fluids not only improve the tribological property but also enhance the viscosity of the based fluids, from which the cutting performance significantly improves. Li, B. et al. [14] studied the heat transfer performance of MQL grinding with different nanofluids for Ni-based alloy. Six types of nanoparticles including MoS<sub>2</sub>, ZrO<sub>2</sub>, CNT, PCD, Al<sub>2</sub>O<sub>3</sub>, SiO<sub>2</sub> were suspended in palm oil to prepare the nanofluids. From the obtained results, the increase of viscosity and thermal conductivity of the base fluid was confirmed when adding nanoparticles. CNT nanofluid has the highest heat transfer coefficient. Hence, the use of nanofluids contributed to reduce the cutting forces and cutting temperature during grinding process. Pil-Ho Lee et al. [15] investigated diamond and Al<sub>2</sub>O<sub>3</sub> nanofluids for MQL micro grinding. The experimental results demonstrated that the grinding forces were much

reduced and the surface quality was significantly improved. The higher volumetric concentration and smaller size of nanoparticle were more effective to decrease the cutting forces. Ali, M.K.A. et al. [16] evaluated the tribological characteristics of  $\text{Al}_2\text{O}_3$  and  $\text{TiO}_2$  nano-lubricant in automotive engines with different concentrations (0.05, 0.1, 0.25 and 0.5 wt %). The decrease in friction coefficient, power losses and wear had been reported. The kinematic viscosity of nano-lubricants decreased slightly, but the viscosity index increased. Especially, the worn surfaces were smoother due to the formation of self-laminating protective films of  $\text{Al}_2\text{O}_3$  nanoparticles. The presence of nanoparticles played an important role in creating the rolling effect to reduce the friction coefficient. Garg, A. et al. [17] studied the effect of nanofluid concentration of MQL micro-drilling process. From the experimental results, the authors pointed out that the nanofluid concentration had the strongest influence on the torque and power consumption. Yıldırım, C. V. and his co-authors [18] recently investigated the effect of hBN nanofluid for MQL turning of Ni-based Inconel 625. The significant enhancement of tool life and surface quality was observed by using hBN nanofluid (0.5 wt %). The results also showed the reduction of cutting temperature and tool wear by using MQL nanofluids when compared to dry machining. Duc, T.M. et al. [19] studied the performance of  $\text{Al}_2\text{O}_3$  nanofluids in MQL hard milling using carbide tools. The experimental results revealed the decrease of friction coefficient, cutting forces and tool wear due to the effectiveness of  $\text{Al}_2\text{O}_3$  nanofluids, which led to the improvement of cutting performance, surface quality, and tool life. Interestingly, the authors also proved that the addition of  $\text{Al}_2\text{O}_3$  nanoparticles in MQL fluids enlarged the applicability of the carbide tools in hard milling while ensuring the proper tool life and achieving the good surface quality, from which the reduction of manufacturing cost can be made. Uysal, A. et al. [20] evaluated the performance of  $\text{MoS}_2$  nanofluid in MQL milling of AISI 420 stainless steel. The results obtained also revealed the reduction in both tool wear and surface roughness due to the lubricating effect of  $\text{MoS}_2$  nanoparticles. Hegab, H. et al. [21,22] studied the turning performance of Ti-6Al-4V alloy under the MQL technique using nano-cutting fluids. By using multi-walled carbon nanotubes (MWCNTs) suspended in vegetable oil, the MQL heat capacity was improved and the power consumption, as well as flank wear, reduced significantly with the nano concentration of 2 wt %. The authors concluded that the cutting performance and surface quality improved due to the interface bonding between the tool and workpiece surface. They also extended the study to investigate the tool performance and chip morphology during machining Inconel 718 by using MWCNTs and  $\text{Al}_2\text{O}_3$  nanofluid [23,24]. The results indicated the enhancement of MQL cooling and lubricating capabilities, which contribute to improve the machining performance compared to the case with no nano-additives. The lower deformed chip thickness was observed, which led to lower cutting forces. Furthermore, a 2-D axisymmetric computational fluid dynamics (CFD) model is developed to simulate the thermal characteristics of nanofluid when machining Ti-6Al-4V and Inconel 718, which was used in the finite element model [25]. This is the first attempt to simulate the MQL machining process using nanofluid. From the obtained results, the improvement of thermal properties and the reduction of friction coefficient were confirmed. The authors also suggested that the negative effect on the tool wear could occur when increasing the nano concentration, but the induced friction could be decreased. Accordingly, the nanofluid concentration should be studied and optimized in order to be applied efficiently to fulfill the technical and economic requirements [26]. Eltaggaz, A. et al. [27,28] investigated the effect on tool life and surface roughness during cutting austempered ductile iron alloys (ADI). Compared to dry, flood, MQL conditions, a significant reduction in the cutting forces and the better surface roughness were reported due to the cooling and lubricating enhancement of gamma- $\text{Al}_2\text{O}_3$  nanofluids. Hence, the lower wear rates and wear levels were observed.

Sharma, A.K. et al. [29] made a review of the effect of MQL in machining processes using conventional and nano cutting fluids. This study covered the important researches regarding the MQL techniques using mineral oils, vegetable oils and nanofluids for different machining processes. From the results, most of the experimental studies had shown better surface quality by using MQL technique with nanofluids when compared to dry and wet cutting. The cutting forces were much reduced due to the rolling effect of nanoparticles suspended in the base fluids. The authors also

suggested focusing on the further studies of the application of MQL with hybrid nanofluids. Singh, R.K. et al. [30] evaluated the performance of alumina-graphene hybrid nanofluid in hard turning. The experimental results revealed that the addition of graphene in alumina nanofluid enhanced the performance of hybrid nanofluids. The reduction of the values of surface roughness and cutting forces was also reported. In addition, the coefficient of friction of hybrid nanofluid was lower when compared to  $\text{Al}_2\text{O}_3$  nanofluid and the base fluid, from which the significant decrease of tool wear was observed. Jamil, M. et al. [31] studied the effects of hybrid  $\text{Al}_2\text{O}_3$ -CNT nano additive-based MQL and cryogenic cooling when machining Ti-6Al-4V alloy. Based on the experimental results, the MQL technique using hybrid nanofluid reduced the values of surface roughness, cutting forces and extended the tool life more effectively than the cryogenic technique. Nevertheless, the cryogenic  $\text{CO}_2$  exhibited heat dissipation efficiently at low cutting speed. Moreover, Sharma, A.K. et al. [32] used alumina- $\text{MoS}_2$  hybrid nanofluid in hard turning of AISI 304 steel. The improvement of tribological properties of hybrid nanofluids was confirmed by experimental results. The thermal conductivity of alumina nanofluid increased by about 9.98%, but the hybridization of  $\text{MoS}_2$  in alumina nanofluid brought out the negative effect with the rise of thermal conductivity by about 8.4%. On the other hand, the increase of temperature and nanoparticle concentration contributed to the improvement of thermal conductivity. The significant reduction of cutting forces and surface roughness had been shown by using the  $\text{Al}_2\text{O}_3$ - $\text{MoS}_2$  hybrid nanofluid when compared to the  $\text{Al}_2\text{O}_3$  nanofluid. The authors also suggested the further studies for investigating the effect of the volumetric ratio of two different nanofluids as well as the optimization of nanoparticle concentration.

From the literature review, it is well documented that the use of nanofluids in MQL hard machining brings out better cutting performance in terms of cutting forces, surface roughness, tool wear, tool life. The main reasons are the improvement of tribological and thermophysical properties of the base fluids when adding nanoparticles. Further studies are necessary for investigating the special properties of nanofluid in order to apply in MQL hard machining more effectively. In addition to that, there are few studies about the effect of alumina and  $\text{MoS}_2$  nanofluids in MQL hard turning in terms of nanoparticle types, nano concentration, and different base fluids. For those reasons, the authors are motivated to conduct MQL hard turning experiments of 90CrSi steel (60–62 HRC) using  $\text{Al}_2\text{O}_3$  and  $\text{MoS}_2$  nanofluids with coated carbide tools. The results of this study will not only provide the important technical guide for using  $\text{Al}_2\text{O}_3$  and  $\text{MoS}_2$  nanoparticles in MQL hard turning, but also be the basis of hybrid nanofluids' applications and development for sustainable production.

## 2. Materials and Methods

### 2.1. Experimental Set up

#### 2.1.1. Experimental Devices

The experimental set up is shown in Figure 1. The CS-460x1000 Chu Shing lathe (Pin Shin Machinery Co., LTD, Taichung city, Taiwan) was used to conduct the experiments. Tungaloy CNMG120404-TM T9125 tungsten carbide inserts with coating layers of CVD  $\text{Al}_2\text{O}_3/\text{TiCN}$  were utilized (Figure 2). Tool holder type with the designation PCLNR 2020 K-16 (KYOCERA Precision Tools, Inc., Kyoto, Japan) was used.

The MQL system includes NOGA MiniCool MC1700 (Noga Engineering & Technology (2008) Ltd, Shlomi, Israel), compressed air, pressure stabilization device, soybean oil, water-based emulsion 5% and  $\text{Al}_2\text{O}_3$  and  $\text{MoS}_2$  nanoparticles. Measuring equipment consists of Kistler quartz three-component dynamometer 9257BA (Kistler Instruments (Pte) Ltd., Midview, Singapore), SJ-210 (Mitutoyo, Kawasaki, Japan) for surface roughness, data acquisition system A/D DQA N16210 (made by National instruments, Austin, TX, USA), and DASylab 10.0 software. Alumina nanoparticles with the size of 30 nm (average) were made by Soochow Hengqiu Graphene Technology Co., Ltd., Suzhou, China (Figure 3).  $\text{MoS}_2$  nanoparticles with the size of 30 nm (average) were made by Luoyang Tongrun Info Technology Co.,



Ltd., Luoyang, China (Figure 4). In this research, 90CrSi steels with a hardness of 60–62 HRC were used. The workpiece diameter is 40 mm with the chemical composition shown in Table 1.

**Table 1.** Chemical composition in % of 90CrSi steel.

Element	C	Si	Mn	Ni	S	P	Cr	Mo	W	V	Ti	Cu
Weight (%)	0.85–0.95	1.20–1.60	0.30–0.60	Max 0.40	Max 0.03	Max 0.03	0.95–1.25	Max 0.20	Max 0.20	Max 0.15	Max 0.03	Max 0.3

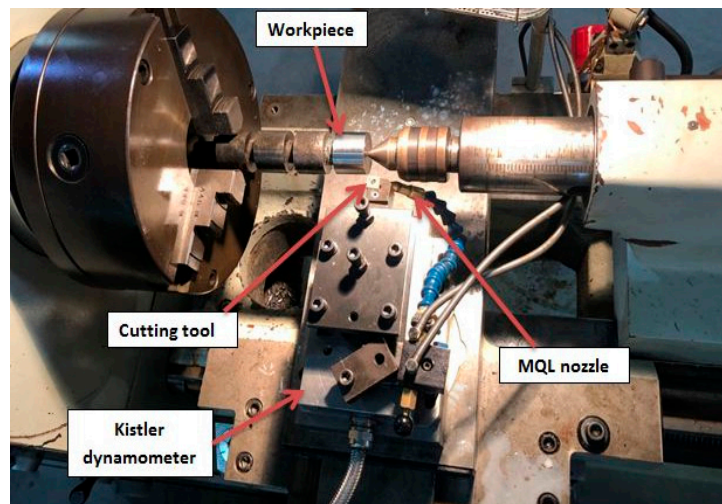


**Figure 1.** The experimental set up.



**Figure 2.** Tungaloy CNMG120404-TM T9125 tungsten carbide inserts.

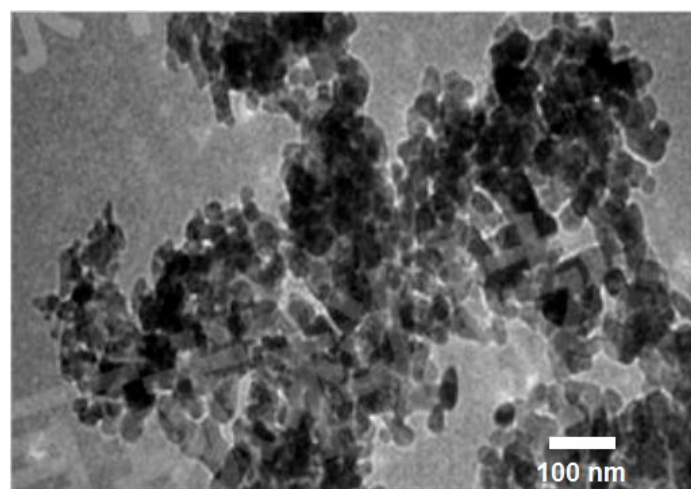


**Figure 3.** Transmission electron microscopy (TEM) image of  $\text{Al}_2\text{O}_3$  nanoparticles [19].

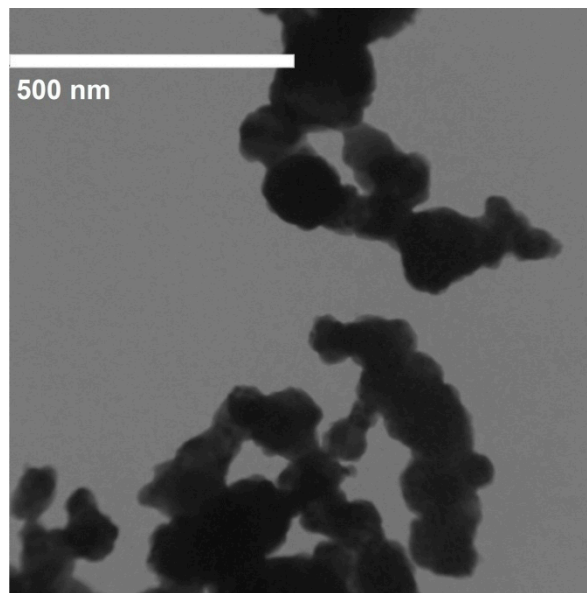


**Figure 4.** TEM image of MoS<sub>2</sub> nanoparticles.

#### 2.1.2. The Preparation of Al<sub>2</sub>O<sub>3</sub> and MoS<sub>2</sub> Nanofluids

The nanoparticle concentration was calculated by the following equation and expressed in weight percent concentration (wt %)

$$\text{Weight percent concentration (wt \%)} = \frac{\text{Weight of solute (g)}}{\text{Weight of solution (g)}} \times 100\% \quad (1)$$

Because the Al<sub>2</sub>O<sub>3</sub> and MoS<sub>2</sub> nanoparticles do not dissolve in soybean oil and water-based emulsion, they will sink to the bottom after a short time. The non-uniform distribution of the nanoparticles will bring out the very little effectiveness on MQL hard machining compared to the base fluids [33]. Another important point is that the nanoparticles in the bottom also cause the waste. To ensure uniform distribution of Al<sub>2</sub>O<sub>3</sub> and MoS<sub>2</sub> nanoparticles in fluids, the prepared nanofluids are kept in Ultrasons-HD ultrasonicator (JP Selecta, Abrera (Barcelona), Spain) (Figure 5), generating 600 W ultrasonic pulses at 40 kHz, and the time for different concentrations 1.0% and 3.0 wt % is at least 40 min, 90 min. to ensure the uniform distribution of the nanoparticles respectively. In order to use the obtained nanofluids effectively and avoid the precipitation of agglomerated nanoparticles during the long time of machining, the nanofluids were placed in the 3000868-Ultrasons-HD and directly used for MQL system.



**Figure 5.** Ultrasons-HD used to generate ultrasonic pulses for the preparation of nanofluids.

### 2.1.3. Experiment Design

The experiment is carried out according to the factorial design  $2^{k-P}$  with four variables ( $k = 4$ ). The factorial design  $N = 2^{k-P}_{IV}$  is chosen, and  $N = 2^{4-1} = 8$ .

Minitab 18 software is used for designing the experiment, and the experimental trials are repeated by 4 times under the same cutting parameters (Table 2). The spindle speeds are chosen as 650 rpm and 950 rpm, which are equivalent to 81.7 m/min and 119.4 m/min, respectively. The experiments are carried out by following the design. The depth of cut and the feed rate are fixed at 0.15 mm and 0.1 mm/rev. The regression model for response parameters is given by:

$$y = b_0 + b_1x_1 + b_2x_2 + \dots + b_nx_n + b_{12}x_1x_2 + b_{13}x_1x_3 + \dots + b_{1n}x_1x_n + \dots + b_{12..n}x_1x_2 \dots x_n \quad (2)$$

**Table 2.** Control factors and their types/levels.

Control factor	Unit	Symbol	Type/Level	Type/Level
Base fluid		$x_1$	Emulsion	Soybean oil
Nanoparticles		$x_2$	$Al_2O_3$	$MoS_2$
Nano concentration (np)	wt %	$x_3$	1	3
Cutting speed	m/min	$x_4$	81.7	119.4

## 3. Results and Discussion

### 3.1. The Effects of Control Factors on the Cutting Forces and Surface Roughness

The results of evaluated responses  $R_a$ ,  $F_x$ ,  $F_y$ ,  $F_z$  are shown in Table 3. ANOVA analysis of MQL parameters for cutting forces  $F_x$ ,  $F_y$ ,  $F_z$  and surface roughness  $R_a$  is given by Tables 4–7 (the symbol \* represents the interactions between the investigated factors). The ANOVA analysis is carried out at a confidence level of 95% (i.e., 5% significance level).

**Table 3.** The design of the experiment with a test run order and output in terms of four response parameters.

Run		Input Machining Parameters				Response Variables			
Std Order	Run Order	Fluid Type	Nano-Particles	np (wt %)	V (m/min)	$R_a$ ( $\mu m$ )	$F_x$ (N)	$F_y$ (N)	$F_z$ (N)
8	1	Soybean	$Al_2O_3$	3	119.4	0.359	43.2	196.5	32.8
26	2	Emulsion	$MoS_2$	1	119.4	1.420	47.9	214	33.9
6	3	Soybean	$MoS_2$	3	81.7	1.212	46.9	214	36.4
7	4	Emulsion	$Al_2O_3$	3	81.7	1.145	36.2	180	34.9
24	5	Soybean	$Al_2O_3$	3	119.4	0.480	43.3	205.7	34.2
12	6	Soybean	$Al_2O_3$	1	81.7	1.378	58.6	164.7	44.0
16	7	Soybean	$Al_2O_3$	3	119.4	0.656	43.0	200.1	32.3
5	8	Emulsion	$MoS_2$	3	119.4	1.170	36.7	222.4	34.7
17	9	Emulsion	$MoS_2$	1	81.7	0.727	35.3	154.3	27.7
2	10	Soybean	$MoS_2$	1	119.4	1.006	49.5	215.3	34.6
19	11	Emulsion	$Al_2O_3$	1	119.4	0.953	30.4	152.4	32.1
11	12	Emulsion	$Al_2O_3$	1	119.4	0.896	32.4	173.2	31.2
29	13	Emulsion	$MoS_2$	3	119.4	1.368	37.7	233.6	34.2
21	14	Emulsion	$MoS_2$	3	119.4	1.439	36.5	226.2	33.1
22	15	Soybean	$MoS_2$	3	81.7	1.350	47.9	213	37.7
20	16	Soybean	$Al_2O_3$	1	81.7	1.026	60.3	173.3	44.4
32	17	Soybean	$Al_2O_3$	3	119.4	0.684	44.6	206.3	33.5

Table 3. Cont.

Run		Input Machining Parameters				Response Variables			
Std Order	Run Order	Fluid Type	Nano-Particles	np (wt %)	V (m/min)	R <sub>a</sub> (μm)	F <sub>x</sub> (N)	F <sub>y</sub> (N)	F <sub>z</sub> (N)
1	18	Emulsion	MoS <sub>2</sub>	1	81.7	1.009	30.8	142.4	30.4
18	19	Soybean	MoS <sub>2</sub>	1	119.4	1.324	56.8	253.4	42.2
14	20	Soybean	MoS <sub>2</sub>	3	81.7	1.240	47.7	210.0	36.7
10	21	Soybean	MoS <sub>2</sub>	1	119.4	1.267	53.7	253.6	44.6
28	22	Soybean	Al <sub>2</sub> O <sub>3</sub>	1	81.7	0.909	41.2	161.3	28.5
23	23	Emulsion	Al <sub>2</sub> O <sub>3</sub>	3	81.7	1.075	36.0	183.3	36.4
4	24	Soybean	Al <sub>2</sub> O <sub>3</sub>	1	81.7	0.824	40.2	164.3	28.6
13	25	Emulsion	MoS <sub>2</sub>	3	119.4	1.425	34.1	230.6	33.5
15	26	Emulsion	Al <sub>2</sub> O <sub>3</sub>	3	81.7	1.103	64.8	181.6	42.9
31	27	Emulsion	Al <sub>2</sub> O <sub>3</sub>	3	81.7	0.984	67.7	208.1	45.5
3	28	Emulsion	Al <sub>2</sub> O <sub>3</sub>	1	119.4	1.124	43.9	177.0	35.0
9	29	Emulsion	MoS <sub>2</sub>	1	81.7	0.625	31.0	163.3	30.9
30	30	Soybean	MoS <sub>2</sub>	3	81.7	0.848	48.8	216.9	38.6
27	31	Emulsion	Al <sub>2</sub> O <sub>3</sub>	1	119.4	0.921	38.4	181.8	32.5
25	32	Emulsion	MoS <sub>2</sub>	1	81.7	0.766	31.6	161.4	31.0

Table 4. Results of ANOVA analysis of the cutting force F<sub>x</sub>.

Source	DF	Adj SS	Adj MS	F-Value	p-Value
Model	7	1701.93	243.13	4.02	<0.005
Linear	4	907.99	227.00	3.75	<0.017
Fluid type	1	704.06	704.06	11.64	<0.002
Nanoparticles	1	82.24	82.24	1.36	0.255
np (wt %)	1	34.24	34.24	0.57	0.459
V (m/min)	1	87.45	87.45	1.45	0.241
2-Way Interactions	3	793.94	264.65	4.38	<0.014
Fluid type * Nanoparticles	1	318.15	318.15	5.26	<0.031
Fluid type * np (wt %)	1	440.30	440.30	7.28	<0.013
Fluid type * V (m/min)	1	35.49	35.49	0.59	0.451
Error	24	1451.70	60.49		
Total	31	3153.64			

Table 5. Results of ANOVA analysis of the cutting force F<sub>y</sub>.

Source	DF	Adj SS	Adj MS	F-Value	p-Value
Model	7	24227.9	3461.12	27.18	<0.000
Linear	4	19934.2	4983.55	39.14	<0.000
Fluid type	1	2642.6	2642.65	20.76	<0.000
Nanoparticles	1	5376.8	5376.84	42.23	<0.000
np (wt %)	1	5581.0	5580.96	43.83	<0.000
V (m/min)	1	6333.8	6333.75	49.75	<0.000
2-Way Interactions	3	4293.7	1431.22	11.24	<0.000
Fluid type * Nanoparticles	1	1529.0	1529.04	12.01	<0.002
Fluid type * np (wt %)	1	2764.0	2763.96	21.71	<0.000
Fluid type * V (m/min)	1	0.7	0.66	0.01	0.943
Error	24	3055.7	127.32		
Total	31	27283.6			

The last column of these tables shows the influence of variation in input variables, and the *p*-values of most of them are smaller than the significance level (0.05). It means that the control factors, such as the type of fluids, the type of nanoparticles, and cutting speed, have a significant influence on the response parameters F<sub>z</sub>, F<sub>y</sub>, F<sub>x</sub> and R<sub>a</sub>. However, the influence of each variable is different, but the cutting force F<sub>y</sub> and surface roughness R<sub>a</sub> are much influenced. The obtained results play an important



role in machining practice because the study objectives are mainly the finish cutting, which requires high accuracy and surface quality. Especially, the cutting force component  $F_y$  has a strong influence on the machining accuracy, so the study for selecting the MQL parameters is necessary to improve the machining accuracy and surface quality.

**Table 6.** Results of ANOVA analysis of the cutting force  $F_z$ .

Source	DF	Adj SS	Adj MS	F-Value	p-Value
Model	7	321.849	45.978	2.56	<0.040
Linear	4	78.645	19.661	1.09	0.382
Fluid type	1	42.781	42.781	2.38	0.136
Nanoparticles	1	2.311	2.311	0.13	0.723
np (wt %)	1	20.801	20.801	1.16	0.293
V (m/min)	1	12.751	12.751	0.71	0.408
2-Way Interactions	3	243.204	81.068	4.51	<0.012
Fluid type * Nanoparticles	1	117.811	117.811	6.56	<0.017
Fluid type * np (wt %)	1	124.031	124.031	6.90	<0.015
Fluid type * V (m/min)	1	1.361	1.361	0.08	0.785
Error	24	431.260	17.969		
Total	31	753.109			

**Table 7.** Results of ANOVA analysis of surface roughness  $R_a$ .

Source	DF	Adj SS	Adj MS	F-Value	p-Value
Model	7	1.89032	0.270045	9.87	<0.000
Linear	4	0.44682	0.111705	4.08	<0.012
Fluid type	1	0.01744	0.017438	0.64	0.433
Nanoparticles	1	0.42297	0.422970	15.46	<0.001
np (wt %)	1	0.00412	0.004118	0.15	0.701
V (m/min)	1	0.00230	0.002295	0.08	0.775
2-Way Interactions	3	1.44350	0.481166	17.58	<0.000
Fluid type * Nanoparticles	1	0.28558	0.285579	10.44	<0.004
Fluid type * np (wt %)	1	0.78532	0.785318	28.70	<0.000
Fluid type * V (m/min)	1	0.37260	0.372600	13.62	<0.001
Error	24	0.65675	0.027365		
Total	31	2.54707			

The regression functions of cutting forces  $F_x$ ,  $F_y$ ,  $F_z$ , and  $R_a$  are given by Equations (3)–(6) with coefficient of determination ( $R^2$ ) equal to 53.97, 88.80, 42.74, and 74.22 respectively.

$$F_x = 43.66 + 4.69x_1 + 1.60x_2 + 1.03x_3 - 1.65x_4 - 3.15x_1x_2 - 3.71x_1x_3 + 1.05x_1x_4 \quad (3)$$

$$F_y = 194.81 + 9.90x_1 - 12.96x_2 + 13.21x_3 + 14.07x_4 - 6.91x_1x_2 - 9.29x_1x_3 + 0.14x_1x_4 \quad (4)$$

$$F_z = 35.281 + 1.156x_1 + 0.269x_2 + 0.806x_3 - 0.631x_4 - 1.919x_1x_2 - 1.969x_1x_3 + 0.206x_1x_4 \quad (5)$$

$$R_a = 1.0223 - 0.0233x_1 - 0.1150x_2 + 0.0113x_3 + 0.0085x_4 - 0.0945x_1x_2 - 0.1567x_1x_3 - 0.1079x_1x_4 \quad (6)$$

The effects of the investigated (input) parameters on the cutting forces are presented in Figures 6–8 and discussed as below:

### 3.1.1. The effect of the fluid type ( $x_1$ )

The type of base fluid has a strong effect on the cutting force components, which are reflected by the slope of the line graph in Figures 6–8. Emulsion-based nanofluid exhibits the smaller values of cutting forces  $F_x$ ,  $F_y$ ,  $F_z$  than those of soybean-based nanofluid. It can be explained that the ignition temperature of soybean oil is lower than that of water-based emulsion. Therefore, the high heat

generated from hard turning makes the lubricating character of soybean oil less effective, and this observation is suitable with previous studies [12,19,34].

### 3.1.2. The effect of the nanoparticle type ( $x_2$ )

The nanoparticle type ( $x_2$ ) also has a strong influence on cutting forces, especially on the thrust force  $F_y$  (shown in Figures 6–8). Interestingly, the results reveal that  $\text{MoS}_2$  nanoparticles exhibit the effectiveness on reducing the cutting forces  $F_x$ ,  $F_z$  but increasing  $F_y$ . In contrast,  $\text{Al}_2\text{O}_3$  nanoparticles exhibit the effectiveness on reducing the cutting force  $F_y$  but increasing  $F_x$ ,  $F_z$ . The main reason is that the morphology of  $\text{Al}_2\text{O}_3$  nanoparticles is nearly spherical with characteristics of high strength, hardness, and heat resistance, which show good abrasive resistance during the friction process and can create the rolling effect to reduce the friction coefficient in contact zone, especially in flank face [35]. Accordingly, the cutting force  $F_y$  significantly reduces. Nevertheless,  $\text{MoS}_2$  nanoparticles are ellipsoidal and provide the low coefficient of friction up to 0.03–0.05 or even lower due to “an easy-to-slide plane” from the weak binding of sulfur atoms between molecular layers [34]. From that,  $\text{MoS}_2$  nanoparticles show the less effect on the cutting force,  $F_y$ , but still effectively in reducing the cutting forces  $F_x$ ,  $F_z$ . In finish hard machining, the cutting force  $F_y$ , which contributes to a strongest influence on the dimensional accuracy. Therefore,  $\text{Al}_2\text{O}_3$  nanoparticles should be used in this case.

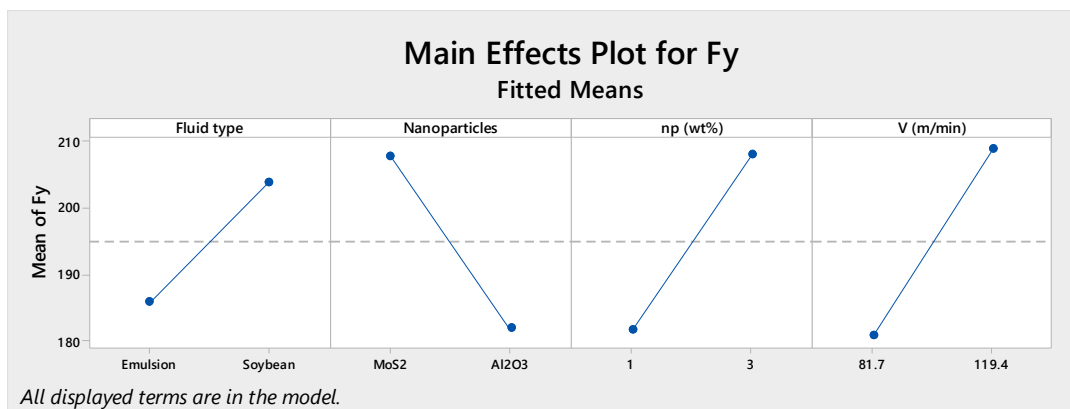


**Figure 6.** Main effect plot for the cutting force  $F_y$ .

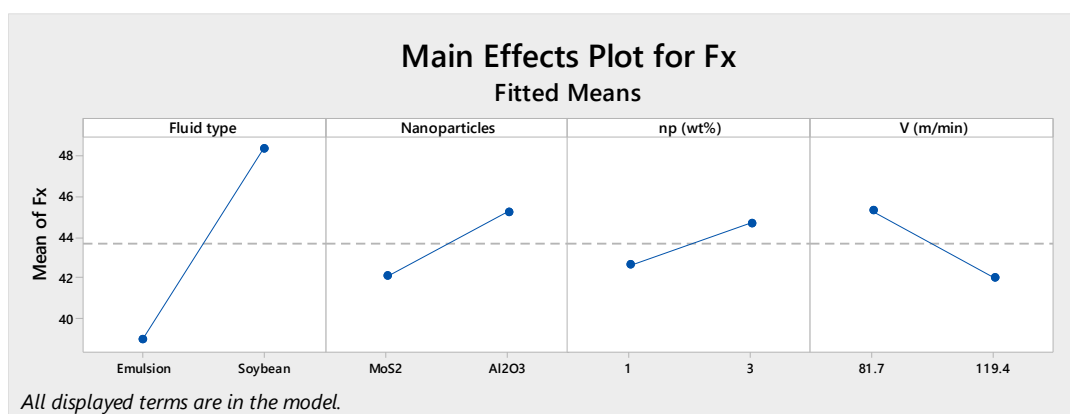


**Figure 7.** Main effect plot for the cutting force  $F_x$ .

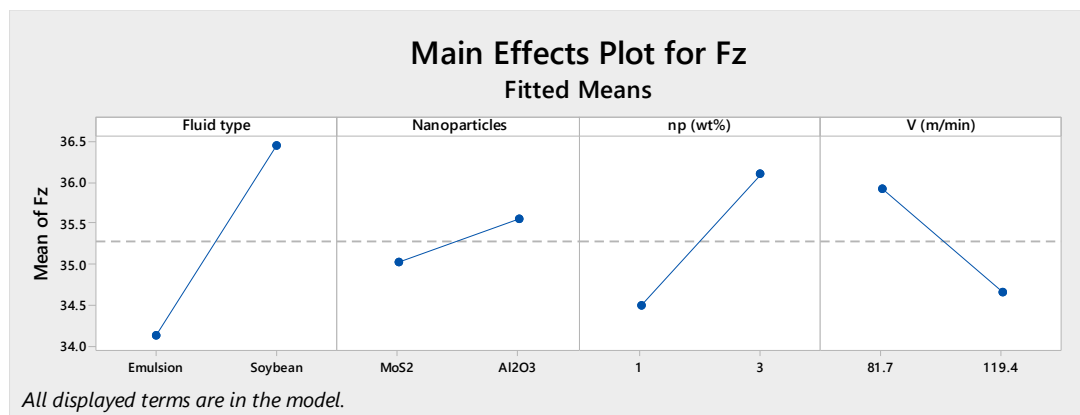


**Figure 8.** Main effect plot for the cutting force  $F_z$ .

### 3.1.3. The effect of the nanoparticle concentration ( $x_3$ )

The nanoparticle concentration exhibits a strong effect on the cutting forces, especially on the thrust force  $F_y$  (shown in Figure 6). The concentration of nanoparticles 1.0 wt % shows more effect on the reduction of cutting forces when compared to the concentration of nanoparticles 3.0 wt %. The proper nanofluid concentration plays a very important role in hard machining. It not only has a significant effect on cutting performance but also contributes to the rise of manufacturing cost. In addition, the use of large nano concentration also causes a negative effect on surface quality [36] and the waste due to the precipitation of nanoparticles. Accordingly, the low nanoparticle concentration should be considered to use for the decrease of cutting forces and to improve the surface quality.

### 3.1.4. The effect of the cutting speed ( $x_4$ )

The cutting speed also exhibits an effect on the cutting forces, especially on the thrust force  $F_y$ . The increase of cutting speed results in the reduction of  $F_x$ ,  $F_z$  and the rise of  $F_y$ . During hard machining, depending on the real cutting condition, the maximum cutting forces always exist at a value of the cutting speed. When rising cutting speed beyond this value, the cutting forces decrease [37]. Accordingly, at the cutting speed  $v = 119.4$  m/min, the cutting force components  $F_x$ ,  $F_z$  go beyond this value, but the cutting force  $F_y$  does not reach it; therefore,  $F_y$  increases. The further studies are needed to extend the results to optimize the cutting speed.

Among the investigated variables including fluid types, the types of nanoparticles, nano concentration and cutting speed, the type of nanoparticles has the strongest influence on  $R_a$ , followed by the fluid types (shown in Figure 9). The Al<sub>2</sub>O<sub>3</sub> nanofluid exhibits smaller values of surface roughness  $R_a$  compared to MoS<sub>2</sub> nanofluid, and the cutting speed has a little effect. The explanation can be concluded that the main effect on surface roughness in hard machining is the geometric factor (the scratch of cutting tools on the machined surface). The dynamic factors concerning with the elastic and plastic deformation of machined surface have little influence. Al<sub>2</sub>O<sub>3</sub> nanoparticles, one of the hexagonal close-packed crystal materials, exhibit the best lubrication performance and are spherical (shown in Figure 3) with characteristics of high hardness. Furthermore, they demonstrate good resistance to high temperature [35,38]. Hence, the “rolling effect” of Al<sub>2</sub>O<sub>3</sub> nanoparticles exhibits the best lubricating performance at cutting zone leading the less scratch on machined surface to improve the surface integrity.

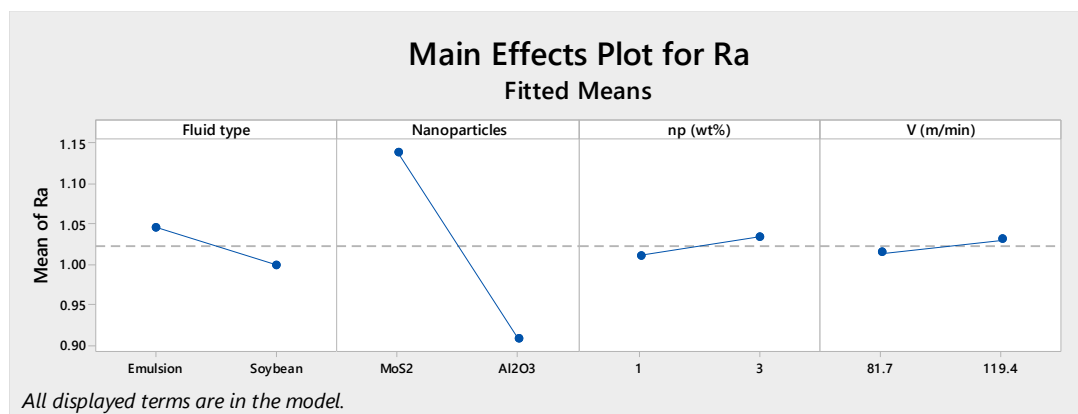


Figure 9. Main effect plot for surface roughness  $R_a$ .

### 3.2. The Interaction Effects among the Investigated Variables

#### 3.2.1. The Interaction Effects of Cutting Force Components $F_x$ , $F_y$ , $F_z$

The interaction effects between the fluid type and the kind of nanoparticles: it can be observed that the values of the objective functions of  $F_x$ ,  $F_y$ ,  $F_z$  increase when changing the base fluid from water-based emulsion to soybean oil, but the increasing amount in case of using MoS<sub>2</sub> nanoparticles is larger than that of using Al<sub>2</sub>O<sub>3</sub> nanoparticles (Figures 10–12). The blue line graph of MoS<sub>2</sub> nanoparticles has a larger slope coefficient than the red one of Al<sub>2</sub>O<sub>3</sub> nanoparticles. It means that the type of nanoparticles has a significant interaction influence on the base fluid type. Then, the combination of using the fluid type and MoS<sub>2</sub> nanoparticles to form the nanofluid has a stronger influence on the cutting force components than using Al<sub>2</sub>O<sub>3</sub> nanoparticles.

The interaction effects between the fluid type and nanoparticle concentration: the nanoparticle concentration has a large interaction effect on the base fluid type, but the increasing amount in case of 1.0 wt % is larger than that of 3.0 wt %, which is reflected by a larger slope coefficient of the blue line graph. Accordingly, the use of the concentration of 1.0 wt % with two base fluids exhibits a stronger influence on cutting forces  $F_x$ ,  $F_y$ ,  $F_z$ .

The interaction effects between the fluid types and cutting speed: from the Figures 10–12, it can be clearly seen that the two line graphs are almost parallel, which means the cutting speed has a very little interacting influence on the two kinds of base fluid.

The other interaction effects with gray backgrounds represent the terms which have very little effect and does not discuss in the investigated model (Figure 10).

#### 3.2.2. The Interaction Effects for Surface Roughness $R_a$

The interaction effects between the fluid type and the kind of nanoparticles: The values of the objective functions of  $F_x$ ,  $F_y$ ,  $F_z$  increase when changing the base fluid from water-based emulsion to soybean oil, which is in contrast to the case of using Al<sub>2</sub>O<sub>3</sub> nanoparticles. In addition, the slope directions of the two line graphs reflect the strong interaction effect on the base fluids. From that, the Al<sub>2</sub>O<sub>3</sub> soybean-based nanofluid should be suggested to achieve the lowest value of surface roughness  $R_a$ .

The interaction effects between the fluid type and nanoparticle concentration are similar to those of the base fluids and cutting speed. The nanoparticle concentration and cutting speed contribute to the strong interacting influence on the kinds of fluid (Figure 13). From the obtained results, to achieve the small values of surface roughness  $R_a$ , the emulsion-based nanofluid with low concentration (1.0 wt %) and cutting speed ( $v = 81.7$  m/min) or the soybean-based nanofluid with high concentration (3.0 wt %) and cutting speed ( $v = 119.4$  m/min) should be used.

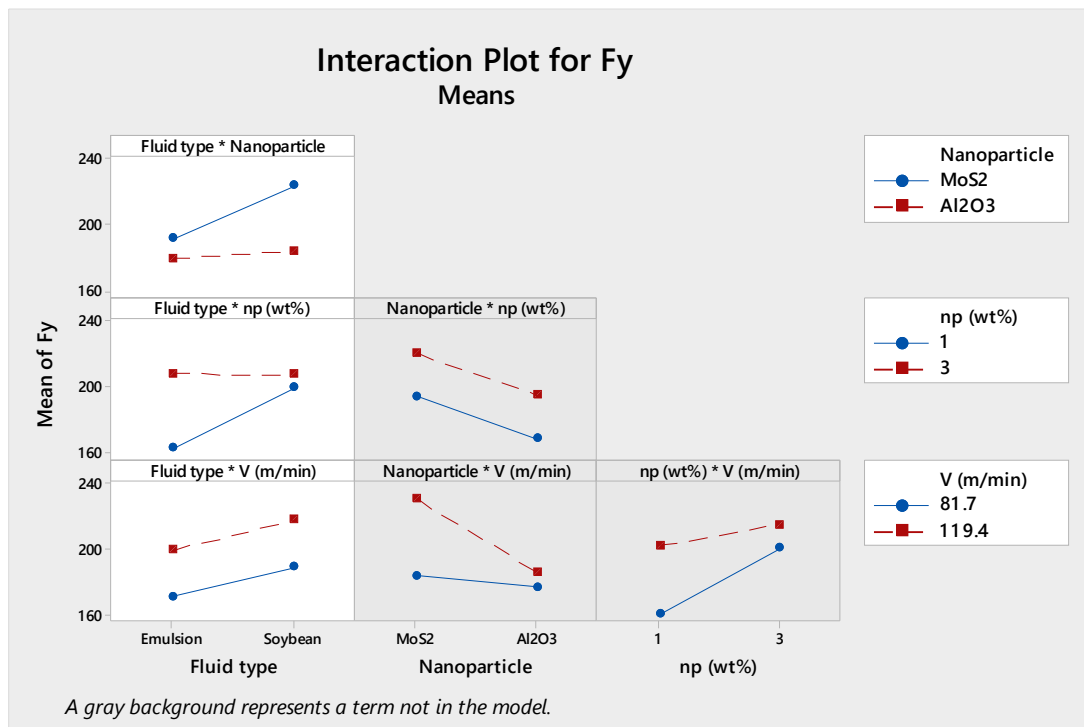


Figure 10. Interaction plot for the cutting force  $F_y$ . \* represents the interactions between the factors.

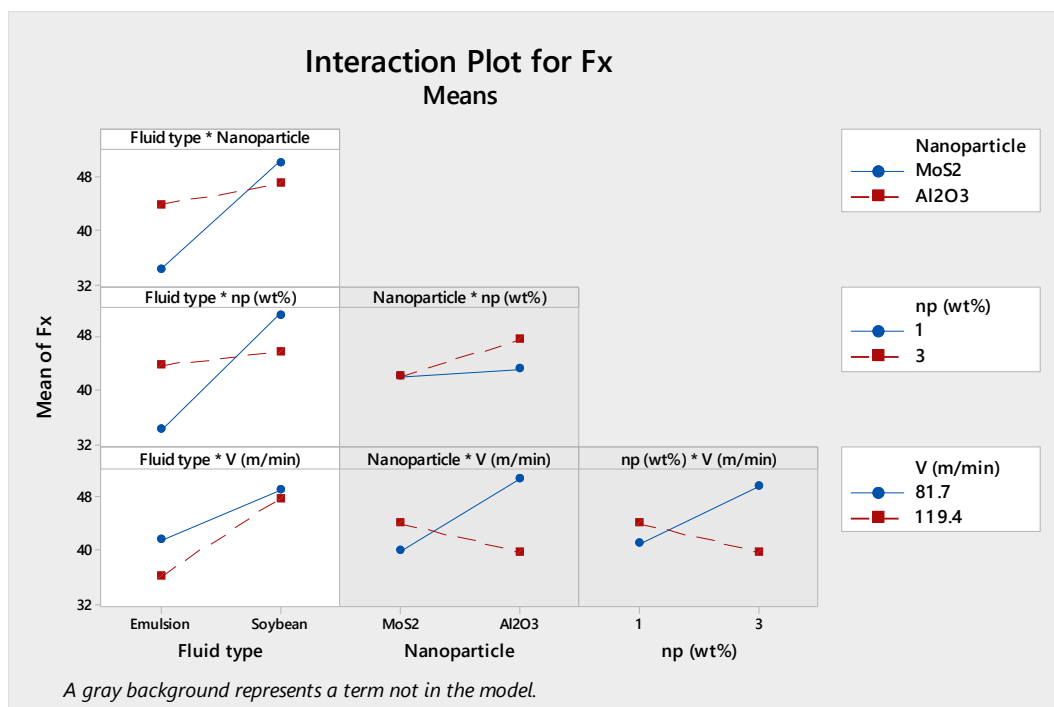


Figure 11. Interaction plot for the cutting force  $F_x$ . \* represents the interactions between the factors.



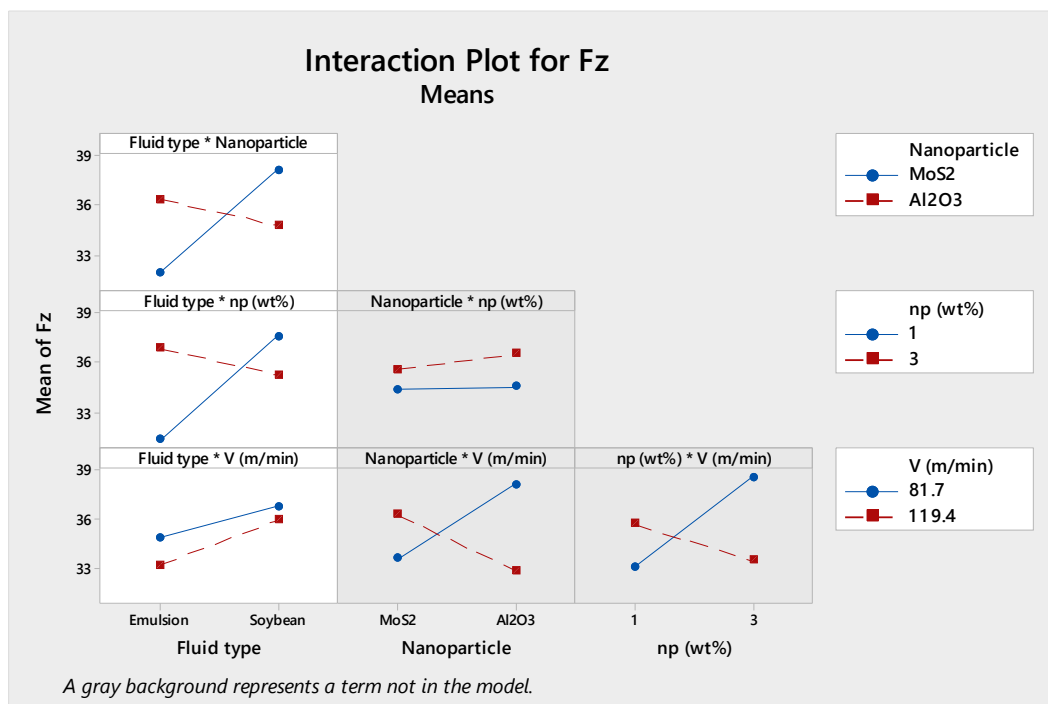


Figure 12. Interaction plot for the cutting force  $F_z$ . \* represents the interactions between the factors.

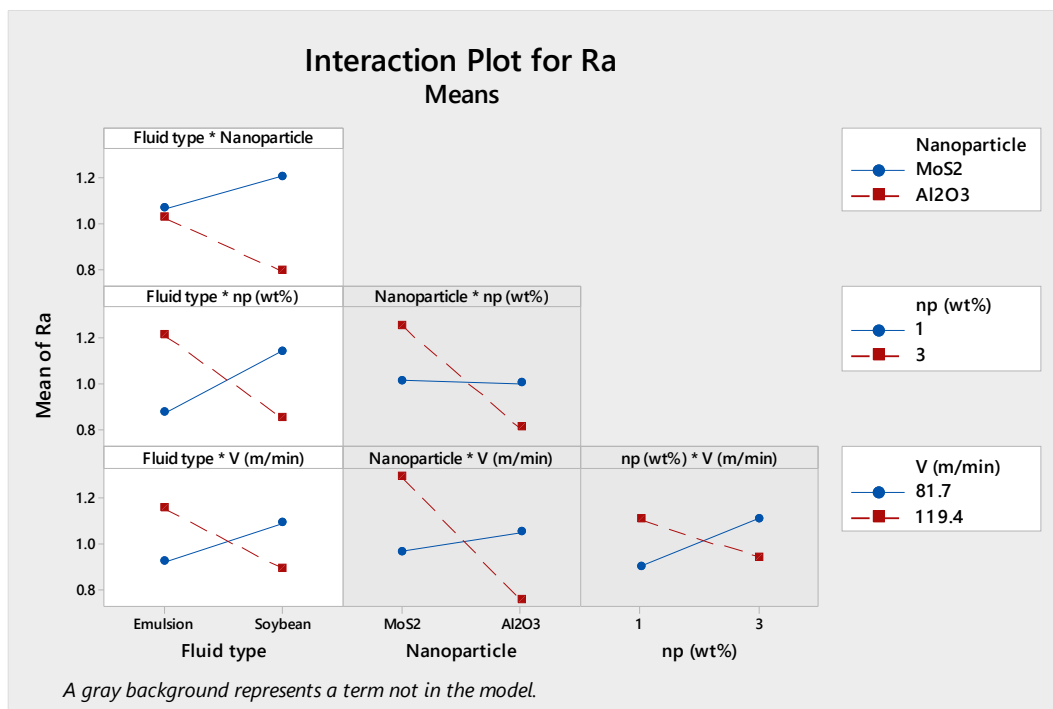


Figure 13. Interaction plot for surface roughness  $R_a$ . \* represents the interactions between the factors.

#### 4. Conclusions

The cutting performance of carbide inserts is improved by the use of the MQL technique with  $Al_2O_3$  and  $MoS_2$  nanofluids. The enhancement of thermal conductivity and lubricating characteristic of the base fluid is observed due to the presence of  $Al_2O_3$  and  $MoS_2$  nanoparticles.

The factorial experimental design is used to evaluate the effects of variables on the objective functions, from which the directions of further studies can be made. In this study, the influence of

MQL parameters, including the fluid types, nanoparticle types, nanoparticle concentration, and cutting speed, is investigated in terms of cutting forces and surface roughness. The obtained results will provide the important direction for selecting the control factors of the further studies.

The empirical regression equations (Equations (2)–(5)) are formulated, and ANOVA analysis is carried out at a confidence level of 95% (i.e., 5% significance level). Most of possibility values ( $p$ -value) are smaller than the significance level  $\alpha = 0.05$ , from which the investigated variables have a significant effect on the objective functions of  $F_x$ ,  $F_y$ ,  $F_z$  and  $R_a$ . In addition, the possibility values of linear models are much smaller than the significance level  $\alpha = 0.05$  and the regression models judged by the coefficients of determination ( $R^2$ ) are suitable.

Based on the experimental results, the direction for MQL parameters using nanofluids is studied in order to reach the desired outputs.  $\text{MoS}_2$  nanofluid has a strong effect on reducing cutting forces  $F_x$ ,  $F_z$  but increasing thrust force ( $F_y$ ), which is contrary to that of  $\text{Al}_2\text{O}_3$  nanofluid. In finish hard turning machining, the thrust force ( $F_y$ ) has a strongest influence on the dimensional accuracy, so  $\text{Al}_2\text{O}_3$  nanofluid should be used in this case. Furthermore, to achieve the lowest value of surface roughness  $R_a$ ,  $\text{Al}_2\text{O}_3$  soybean-based nanofluid shows the better performance than that of the other investigated ones.

The investigation of  $\text{Al}_2\text{O}_3$  and  $\text{MoS}_2$  nanofluids for MQL hard turning will provide the necessary technical guideline on using nanofluids and hybrid nanofluid more efficiently.

In further research, more investigations need to be focused on the effects of the concentration and size of nanoparticles and their interaction with the fluid types on tribological and heat transfer mechanisms in hard machining. The influence of nanoparticle morphology is necessary to be performed to understand the interaction with the friction coefficient. In addition, more focus will be given to optimize the parameter of  $\text{Al}_2\text{O}_3$  and  $\text{MoS}_2$  nanofluid.

**Author Contributions:** Conceptualization, T.M.D.; Data curation, T.T.L. and T.Q.C.; Formal analysis, T.M.D. and T.T.L.; Investigation, T.T.L. and T.Q.C.; Methodology, T.Q.C.; Software, T.Q.C.; Supervision, T.M.D.; Visualization, T.Q.C.; Writing—original draft, T.M.D. and T.T.L.; Writing—review & editing, T.T.L.

**Funding:** This research was funded by Thai Nguyen University of Technology, Thai Nguyen University, Vietnam with the project number of T2018-B05.

**Conflicts of Interest:** The authors declare no conflict of interest.

## References

1. Davim, J.P. *Machining of Hard Materials*; Springer-Verlag London Limited: London, UK, 2011.
2. Zhang, K.; Deng, J.; Meng, R.; Gao, P.; Yue, H. Effect of nano-scale textures on cutting performance of WC/Co-based Ti55Al45N coated tools in dry cutting. *Int. J. Refract. Metals Hard Mater.* **2015**, *51*, 35–49. [[CrossRef](#)]
3. Liu, Y.; Deng, J.; Wang, W.; Duan, R.; Meng, R.; Ge, D.; Li, X. Effect of texture parameters on cutting performance of flank-faced textured carbide tools in dry cutting of green  $\text{Al}_2\text{O}_3$  ceramics. *Ceram. Int.* **2018**, *44*, 13205–13217. [[CrossRef](#)]
4. Kumar, C.S.; Patel, S.K. Effect of WEDM surface texturing on  $\text{Al}_2\text{O}_3$  /TiCN composite ceramic tools in dry cutting of hardened steel. *Ceram. Int.* **2018**, *44*, 2510–2523. [[CrossRef](#)]
5. Xing, Y.; Deng, J.; Zhao, J.; Zhang, G.; Zhang, K. Cutting performance and wear mechanism of nanoscale and microscale textured  $\text{Al}_2\text{O}_3$ /TiC ceramic tools in dry cutting of hardened steel. *Int. J. Refract. Metals Hard Mater.* **2014**, *43*, 46–58. [[CrossRef](#)]
6. Su, Y.; Li, Z.; Li, L.; Wang, J.; Gao, H.; Wang, G. Cutting performance of micro-textured polycrystalline diamond tool in dry cutting. *J. Manuf. Process.* **2017**, *27*, 1–7. [[CrossRef](#)]
7. Bouacha, K.; Yallese, M.A.; Mabrouki, T.; Rigal, J.-F. Statistical analysis of surface roughness and cutting forces using response surface methodology in hard turning of AISI 52100 bearing steel with CBN tool. *Int. J. Refract. Metals Hard Mater.* **2010**, *28*, 349–361. [[CrossRef](#)]
8. Rahim, E.A.; Dorairaju, H. Evaluation of mist flow characteristic and performance in Minimum Quantity Lubrication (MQL) machining. *Measurement* **2018**, *123*, 213–225. [[CrossRef](#)]

9. Abdul Sani, A.S.; Rahim, E.A.; Sharif, S.; Sasahara, H. Machining performance of vegetable oil with phosphonium- and ammonium-based ionic liquids via MQL technique. *J. Clean. Prod.* **2018**, *209*, 947–964. [[CrossRef](#)]
10. Joshi, K.K.; Kumar, R.; Anurag. An Experimental Investigations in Turning of Incoloy 800 in Dry, MQL and Flood Cooling Conditions. *Procedia Manuf.* **2018**, *20*, 350–357. [[CrossRef](#)]
11. Tunc, L.T.; Gu, Y.; Burke, M.G. Effects of Minimal Quantity Lubrication (MQL) on Surface Integrity in Robotic Milling of Austenitic Stainless Steel. *Procedia CIRP* **2016**, *45*, 215–218. [[CrossRef](#)]
12. Minh, D.T.; The, L.T. Investigation of MQL-Employed Hard-Milling Process of S60C Steel Using Coated-Cemented Carbide Tools. *J. Mech. Eng. Autom.* **2016**, *6*, 128–132.
13. Kang, M.C.; Kim, K.H.; Shin, S.H.; Jang, S.H.; Park, J.H.; Kim, C. Effect of the minimum quantity lubrication in high-speed end-milling of AISI D2 cold-worked die steel (62 HRC) by coated carbide tools. *Surf. Coat. Technol.* **2008**, *202*, 5621–5624. [[CrossRef](#)]
14. Li, B.; Li, C.; Zhang, Y.; Wang, Y.; Jia, D.; Yang, M.; Sun, K. Heat transfer performance of MQL grinding with different nanofluids for Ni-based alloys using vegetable oil. *J. Clean. Prod.* **2017**, *154*, 1–11. [[CrossRef](#)]
15. Lee, P.-H.; Nam, J.S.; Li, C.; Lee, S.W. An Experimental Study on Micro-Grinding Process with Nanofluid Minimum Quantity Lubrication (MQL). *Int. J. Precis. Eng. Manuf.* **2012**, *13*, 331–338. [[CrossRef](#)]
16. Ali, M.K.A.; Xianjun, H.; Mai, L.; Qingping, C.; Turkson, R.F.; Bicheng, C. Improving the tribological characteristics of piston ring assembly in automotive engines using Al<sub>2</sub>O<sub>3</sub> and TiO<sub>2</sub> nanomaterials as nanolubricant additives. *Tribol. Int.* **2016**, *103*, 540–554. [[CrossRef](#)]
17. Garg, A.; Sarma, S.; Panda, B.N.; Zhang, J.; Gao, L. Study of effect of nanofluid concentration on response characteristics of machining process for cleaner production. *J. Clean. Prod.* **2016**, *135*, 476–489. [[CrossRef](#)]
18. Yıldırım, Ç.V.; Sarıkaya, M.; Kivak, T.; Şirin, Ş. The effect of addition of hBN nanoparticles to nanofluid-MQL on tool wear patterns, tool life, roughness and temperature in turning of Ni-based Inconel 625. *Tribol. Int.* **2019**, *134*, 443–456. [[CrossRef](#)]
19. Minh, D.T.; The, L.T.; Bao, N.T. Performance of Al<sub>2</sub>O<sub>3</sub> nanofluids in minimum quantity lubrication in hard milling of 60Si<sub>2</sub>Mn steel using cemented carbide tools. *Adv. Mech. Eng.* **2017**, *9*, 1–9. [[CrossRef](#)]
20. Uysal, A.; Demiren, F.; Altan, E. Applying Minimum Quantity Lubrication (MQL) Method on Milling of Martensitic Stainless Steel by Using Nano MoS<sub>2</sub> Reinforced Vegetable Cutting Fluid. *Procedia Soc. Behav. Sci.* **2015**, *195*, 2742–2747. [[CrossRef](#)]
21. Hegab, H.; Umer, U.; Deiab, I.; Kishawy, H. Performance evaluation of Ti–6Al–4V machining using nano-cutting fluids under minimum quantity lubrication. *Int. J. Adv. Manuf. Technol.* **2018**, *95*, 4229–4241. [[CrossRef](#)]
22. Hegab, H.; Kishawy, H.A.; Gadallah, M.H.; Umer, U.; Deiab, I. On machining of Ti-6Al-4V using multi-walled carbon nanotubes-based nano-fluid under minimum quantity lubrication. *Int. J. Adv. Manuf. Technol.* **2018**, *97*, 1593–1603. [[CrossRef](#)]
23. Hegab, H.; Umer, U.; Soliman, M.; Kishawy, H.A. Effects of nano-cutting fluids on tool performance and chip morphology during machining Inconel 718. *Int. J. Adv. Manuf. Technol.* **2018**, *96*, 3449–3458. [[CrossRef](#)]
24. Hegab, H.; Kishawy, H. Towards Sustainable Machining of Inconel 718 Using Nano-Fluid Minimum Quantity Lubrication. *J. Manuf. Mater. Process.* **2018**, *2*, 50. [[CrossRef](#)]
25. Hegab, H.; Kishawy, H.A.; Umer, U.; Mohany, A. A model for machining with nano-additives based minimum quantity lubrication. *Int. J. Adv. Manuf. Technol.* **2019**. [[CrossRef](#)]
26. Hegab, H.; Darras, B.; Kishawy, H.A. Sustainability Assessment of Machining with Nano-Cutting Fluids. *Procedia Manuf.* **2018**, *26*, 245–254. [[CrossRef](#)]
27. Eltaggaz, A.; Zawada, P.; Hegab, H.A.; Deiab, I.; Kishawy, H.A. Coolant strategy influence on tool life and surface roughness when machining ADI. *Int. J. Adv. Manuf. Technol.* **2017**, *94*, 3875–3887. [[CrossRef](#)]
28. Eltaggaz, A.; Hegab, H.; Deiab, I.; Kishawy, H.A. Hybrid nano-fluid-minimum quantity lubrication strategy for machining austempered ductile iron (ADI). *Int. J. Interact. Des. Manuf.* **2018**, *12*, 1273–1281. [[CrossRef](#)]
29. Sharma, A.K.; Tiwari, A.K.; Dixit, A.R. Effects of Minimum Quantity Lubrication (MQL) in machining processes using conventional and nanofluid based cutting fluids: A comprehensive review. *J. Clean. Prod.* **2016**, *127*, 1–18. [[CrossRef](#)]
30. Singh, R.K.; Sharma, A.K.; Dixit, A.R.; Tiwari, A.K.; Pramanik, A.; Mandal, A. Performance evaluation of alumina-graphene hybrid nano-cutting fluid in hard turning. *J. Clean. Prod.* **2017**, *162*, 830–845. [[CrossRef](#)]

31. Jamil, M.; Khan, A.M.; Hegab, H.; Gong, L.; Mia, M.; Gupta, M.K.; He, N. Effects of hybrid Al<sub>2</sub>O<sub>3</sub>-CNT nanofluids and cryogenic cooling on machining of Ti-6Al-4V. *Int. J. Adv. Manuf. Technol.* **2019**. [[CrossRef](#)]
32. Sharma, A.K.; Singh, R.K.; Dixit, A.R.; Tiwari, A.K. Novel uses of alumina-MoS<sub>2</sub> hybrid nanoparticle enriched cutting fluid in hard turning of AISI 304 steel. *J. Manuf. Process.* **2017**, *30*, 467–482. [[CrossRef](#)]
33. Huang, W.-T.; Liu, W.-S.; Tsai, J.-T.; Chou, J.-H. Multiple Quality Characteristics of Nanofluid/Ultrasonic Atomization Minimum Quality Lubrication for Grinding Hardened Mold Steel. *IEEE Trans. Autom. Sci. Eng.* **2018**, *15*, 1065–1077. [[CrossRef](#)]
34. Long, T.T.; Duc, T.M. Micro/Nanofluids in Sustainable Machining. In *Microfluidics and Nanofluidics*, 1st ed.; Sheikholeslami, M., Ed.; Intech Open: London, UK, 2018; pp. 161–199. ISBN 978-1-78923-541-8.
35. Luo, T.; Wein, X.; Huang, X.; Huang, L.; Yang, F. Tribological properties of Al<sub>2</sub>O<sub>3</sub> nanoparticles as lubricating oil additives. *Ceram. Int.* **2014**, *40*, 7143–7149. [[CrossRef](#)]
36. Lee, G.J.; Park, J.J.; Lee, M.K.; Rhee, C.K. Stable dispersion of nanodiamonds in oil and their tribological properties as lubricant additives. *Appl. Surf. Sci.* **2017**, *415*, 24–27. [[CrossRef](#)]
37. Ebrahimi, A.; Moshksar, M.M. Evaluation of machinability in turning of microalloyed and quenched-tempered steels: Tool wear, statistical analysis, chip morphology. *J. Mater. Process. Technol.* **2009**, *209*, 910–921. [[CrossRef](#)]
38. Wang, Y.; Li, C.; Zhang, Y.; Li, B.; Yang, M.; Zhang, X.; Guo, S.; Liu, G. Experimental evaluation of the lubrication properties of the wheel/workpiece interface in MQL grinding with different nanofluids. *Tribol. Int.* **2016**, *99*, 198–210. [[CrossRef](#)]



© 2019 by the authors. Licensee MDPI, Basel, Switzerland. This article is an open access article distributed under the terms and conditions of the Creative Commons Attribution (CC BY) license (<http://creativecommons.org/licenses/by/4.0/>).